Title

Structural basis for altered positional specificity of 15-lipoxygenase-1 with 5S-HETE and 7S-HDHA and the implications for the biosynthesis of resolvin E4

Authors

Perry, Steven C
van Hoorebeke, Christopher
Sorrentino, James
et al.

Publication Date

2022-09-01

DOI

10.1016/j.abb.2022.109317

Structural basis for altered positional specificity of 15-Lipoxygenase-1 with 5S-HETE and 7S-HDHA and the implications for the biosynthesis of Resolvin E4

Steven C. Perry,[#] Christopher van Hoorebeke,[#] James Sorrentino, Leslie Bautista, Oluwayomi Akinkugbe, William S. Conrad, Natalie Rutz, Theodore R. Holman[*]

[1]Department of Chemistry and Biochemistry, University of California Santa Cruz

[#]These authors contributed equally to this publication.
*****To whom correspondence should be addressed: Theodore R. Holman, Department of Chemistry and Biochemistry, University of California Santa Cruz, Santa Cruz, CA 95064; holman@ucsc.edu; Tel.: +1(831) 459-5884; fax: +1(831)459-2935

FUNDING: NIH R01 GM105671

Abstract

Human 15-lipoxygenases (LOX) are critical enzymes in the inflammatory process, producing various pro-resolution molecules, such as lipoxins and resolvins, but the exact role each of the two 15-LOXs in these biosynthetic pathways remains elusive. Previously, it was observed that h15-LOX-1 reacted with 5S-HETE in a non-canonical manner, producing primarily the 5S,12S-diHETE product. To determine the active site constraints of h15-LOX-1 in achieving this reactivity, amino acids involved in the fatty acid binding were investigated. It was observed that R402L did not have a large effect on 5S-HETE catalysis, but F414 appeared to π–π stack with 5S-HETE, as seen with AA binding, indicating an aromatic interaction between a double bond of 5S-HETE and F414. Decreasing the size of F352 and I417 shifted oxygenation of 5S-HETE to C12, while increasing the size of these residues reversed the positional specificity of 5S-HETE to C15. Mutants at these locations demonstrated a similar effect with 7S-HDHA as the substrate, indicating that the depth of the active site regulates product specificity for both substrates. Together, these data indicate that of the three regions proposed to control positional specificity, π–π stacking and active site cavity depth are the primary determinants of positional specificity with 5S-HETE and h15-LOX-1. Finally, the altered reactivity of h15-LOX-1 was also observed with 5S-HEPE, producing 5S,12S-diHEPE instead of 5S,15S-diHEPE (aka resolvin E_4 (RvE_4). However, h15-LOX-2 efficiently produces 5S,15S-diHEPE from 5S-HEPE. This result is important with respect to the biosynthesis of the RvE_4 since it obscures which LOX isozyme is involved in its biosynthesis. Future work detailing the expression levels of the lipoxygenase isoforms in immune cells and selective inhibition during the inflammatory response will be required for a comprehensive understanding of RvE_4 biosynthesis.

Abbreviations

AA, arachidonic acid

d_8-AA, 5Z,8Z,11Z,14Z-eicosatetraenoic-5,6,8,9,11,12,14,15-d_8 acid

DHA, docosahexaenoic acid

EPA, eicosapentaenoic acid

Maresin 1, MaR1, 7R,14S-dihydroxy-4Z,8E,10E,12Z,16Z,19Z docosahexaenoic acid

SPM, specialized pro-resolving mediators

PUFA, polyunsaturated fatty acids

13S-HODE, 13*S*-hydroxy-9*Z*,11*E*-octadecadienoic acid

5S-HETE, 5S-hydroxy-6E,8Z,11Z,14Z-eicosatetraenoic acid

5S-HpETE, 5S-hydroperoxy-6E,8Z,11Z,14Z-eicosatetraenoic acid

15S-HETE, 15S-hydroxy-5Z,8Z,11Z,13E-eicosatetraenoic acid

15S-HpETE, 15S-hydroperoxy-5Z,8Z,11Z,13E-eicosatetraenoic acid

5S,12S-diHETE, 5S,12S-dihydroxy-6E,8Z,10E,14Z-eicosatetraenoic acid

5S,15S-diHETE, 5S,15S-dihydroxy-6E,8Z,11Z,13E-eicosatetraenoic acid

5S-HEPE, 5S-hydroxy-6E,8Z,11Z,14Z,17Z-eicosapentaenoic acid

5S-HpEPE, 5S-hydroperoxy-6E,8Z,11Z,14Z,17Z-eicosapentaenoic acid

15S-HEPE, 15S-hydroxy-5Z,8Z,11Z,13E,17Z-eicosapentaenoic acid

15S-HpEPE, 15S-hydroperoxy-5Z,8Z,11Z,13E,17Z-eicosapentaenoic acid

5S,12S-diHEPE, 5S,12S-dihydroxy-6E,8Z,10E,14Z,17Z-eicosapentaenoic acid

5S,15S-diHEPE, 5S,15S-dihydroxy-6E,8Z,11Z,13E,17Z-eicosapentaenoic acid

7S-HDHA, 7S-hydroxy-4Z,8E,10Z,13Z,16Z,19Z-docosahexaenoic acid

7S-HpDHA, 7S-hydroperoxy-4Z,8E,10Z,13Z,16Z,19Z-docosahexaenoic acid

7S,14S-diHDHA, 7S,14S-dihydroxy-4Z,8E,10Z,12E,16Z,19Z-docosahexaenoic acid

7S,17S-diHDHA, 7S,17S-dihydroxy-4Z,8E,10Z,13Z,15E,19Z-docosahexaenoic acid

Resolvin D_5, RvD_5 (7S,17S-diHDHA)

Resolvin E_4, RvE_4, (5S,15S-diHEPE)

LOX, lipoxygenases

h15-LOX-1, human 15-lipoxygenase-1

h5-LOX, human 5-lipoxygenase

h15-LOX-2, human epithelial 15-lipoxygenase-2

h12-LOX, human platelet 12-lipoxygenase

r15-LOX, rabbit 15-lipoxygenase

FLAP, 5-lipoxygenase activating protein

Introduction

Lipoxygenases (LOXs) are non-heme iron-containing dioxygenases that catalyze the hydroperoxidation of polyunsaturated acids (PUFA) containing a 1,4-pentadiene moiety[1, 2] and play an important role in regulating the process of inflammation.[3, 4] They can react with a variety of dietary fatty acids to form products broadly classified as oxylipins. Specialized-pro-resolving mediators (SPM) are a type of oxylipin that regulate the switch from a pro-inflammatory to a pro-resolving state[5, 6], with oxylipins derived from ω-3 fatty acids, such as eicosapentaenoic acid (EPA) and docosahexaenoic acid (DHA), having a larger role in pro-resolution than that of the ω-6 fatty acid, arachidonic acid (AA). LOXs can produce both pro–inflammatory mediators such as the leukotrienes, as well as anti-inflammatory SPM, such as the lipoxins, resolvins and maresins.[7]

The stereo- and regio-specificity of LOXs determine which oxylipin mediators a cell may produce, either on their own or in concert with other LOX isozymes expressed in neighboring cells through the process of transcellular biosynthesis.[8] h15-LOX-1 is one of two 15-LOXs found in humans[9]. No crystal structure of h15-LOX-1 is available, so most studies to date have attempted to understand the stereo- and regio-specificity of the enzyme by comparison to the structures of rabbit 15-LOX (r15-LOX) and human platelet 12-lipoxygenase (h12-LOX)[10, 11]. h15-LOX-1 shares 81% identity with r15-LOX (95% similarity), 65% identity to h12-LOX (88% similarity), but only 38% identity with h15-LOX-2 (72% similarity). In addition, if the critical active site residues are compared between h15-LOX-1 and h15-LOX-2, a low sequence identity of 47% is still observed.

15-LOXs principally catalyze the abstraction of a hydrogen from C13 of AA followed by insertion of dioxygen onto C15. The resulting molecule is 15S-hydroperoxy-5Z,8Z,11Z,13E-eicosatetraenoic acid (15S-HpETE), which can be reduced by glutathione peroxidases to 15S-hydroxy-5Z,8Z,11Z,13E-eicosatetraenoic acid (15S-HETE).[12,13] The location of hydrogen abstraction depends on the depth of insertion of the methyl end of the substrate and which bis-allylic carbon is located proximal to the enzymes' active site iron. Generally, h15-LOX-1 abstracts the hydrogen atom from the ω-8 carbon, with oxygenation at the ω-6 carbon, with a smaller percentage of the ω-9 product also being made.[14] With AA and the ω-3 PUFA, EPA, the enzyme produces approximately 85% of the 15-product (ω-6) and 15% of the 12-product (ω-9)[15, 16]. In contrast, h15-LOX-2

produces approximately 100% of the 15-oxylipin product with AA as substrate, giving it a more stringent criteria for product formation. However, placing a hydroxyl group on C5 of AA or C7 of DHA changes the product profile of h15-LOX-1 with these substrates[15, 17]. For example, h15-LOX-1 shows a shift in the product profile when 5S-hydroxy-6E,8Z,11Z,14Z-eicosatetraenoic acid (5S-HETE) is the substrate, producing a 14:86 ratio of the ω-6 and ω-9 products. This indicates that the location of hydrogen abstraction is shifted from C13 with AA to C10 with 5S-HETE. A similar shift in product profile emerges when h15-LOX-1 reacts with the DHA oxylipin, 7S-hydroxy-4Z,8E,10Z,13Z,16Z,19Z-docosahexaenoic acid (7S-HDHA). In this case, h15-LOX-1 reacts with DHA to produce 67% of the 17-product (ω-6) and 20% of the 14-product (ω-9) but reacts with 7S-HDHA to produce 10% of the 17-product (ω-6) and 90% of the 14-product (ω-9) (a ratio of 10:90 for the ω-6:ω-9 products), similar to that see with 5S-HETE as the substrate[17]. In contrast, h15-LOX-2 produces almost 100% of the ω-6 di-oxygenated product[15, 17] with either 5S-HETE or 7S-HDHA as substrates.

Altered product specificity has important implications for the biosynthesis of SPM. The proposed biosynthetic routes of SPM, such as 5S,15S-6E,8Z,11Z,13E-dihydroxyeicosatetraenoic acid (5S,15S-diHETE), resolvin E4 (RvE_4, 5S,15S-dihydroxy-6E,8Z,11Z,13E,17Z-eicosapentaenoic acid, 5S,15S-diHEPE) and resolvin D5 (RvD_5, 7S,17S-dihydroxy-4Z,8E,10Z,13Z,15E,19Z-docosahexaenoic acid, 7S,17S-diHDHA), are based on the positional specificity of h15-LOX-1 with fatty acids, such as AA, EPA or DHA.[18,19, 20] However, the altered positional specificity of h15-LOX-1 with oxylipins suggests that h15-LOX-2 may be involved in the production of 5S,15S-diHETE, RvD_5 and RvE_4, due to its aforementioned higher fidelity. h15-LOX-1 instead produces 5S,12S-dihydroxy-6E,8Z,10E,14Z-eicosatetraenoic acid (5S,12S-diHETE), 5S,12S-dihydroxy-6E,8Z,10E,14Z,17Z-eicosapentaenoic acid (5S,12S-diHEPE), and 7S,14S-dihydroxy-4Z,8E,10Z,12E,16Z,19Z-docosahexaenoic acid (7S,14S-diHDHA) (**Figure 1**). Therefore, the *in vivo* biosynthetic routes of these molecules should be carefully evaluated with the altered positional specificity of h15-LOX-1 and the higher fidelity of h15-LOX-2 in mind.

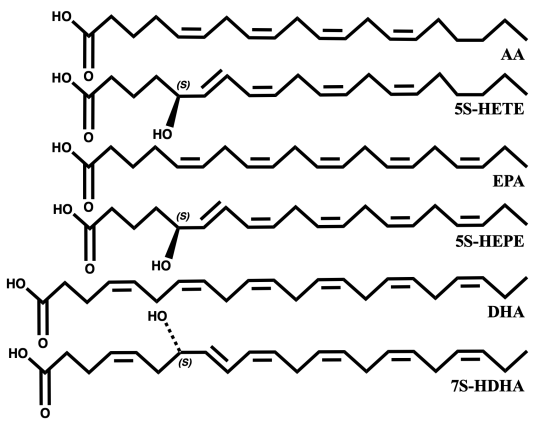

Figure 1. Structures of AA, EPA, DHA and their primary h5-LOX oxylipin products.

As stated above, the altered positional specificity of h15-LOX-1 is unusual, as it does not occur in other LOXs. h15-LOX-2, for example, shows strict regiospecificity. It produces approximately 100% the ω-6 product with AA, DHA, 5S-HETE and 7S-HDHA as the substrates[15, 17, 21]. Similarly, h12-LOX produces approximately 100% of the ω-9 product from AA and greater than 90% of the ω-9 product from 5S-HETE. This suggests that distinct active site structural features of h15-LOX-1 lead to its altered positional specificity.

The structural basis for the stereo- and regio-specificity of h15-LOX-1 with AA has been investigated using site-directed mutagenesis of the active site. Three regions of the active site have been shown to be important for determining the positional specificity of h15-LOX-1 **(Figure 2)**[22]. Early work established that the aromatic ring of F414 forms a π–π stacking interaction with the substrate's Δ11 double bond and that R402 interacts with the terminal carboxylate[10, 23-26]. Sloane and coworkers also demonstrated that I417 and M418 help define the bottom of the active site cavity and that mutating these residues to smaller amino acids allowed the substrate to slide deeper into the active site, causing the enzyme to produce more 12-product (ω-9)[10]. Kuhn and coworkers expanded this work by showing that F352 further defines the active site and aids in maintaining C15 oxygenation over C12 oxygenation[27-30]. These studies lead to the fatty acid binding hypothesis, in which the specificity of the active site is defined by a few critical amino acids: I417 and M418 at the bottom of the active site, R402 at the active site entrance, and F414 and F352 in the middle of the active site[31]. These residues are positioned along in the boot-shaped active site cavity into which the substrate enters methyl-end first. This

model is also observed with structural studies of h12-LOX, in which analogous mutations of conserved amino acids produced similar effects to those seen in h15-LOX-1, albeit with minimal arginine interaction at the entrance[11].

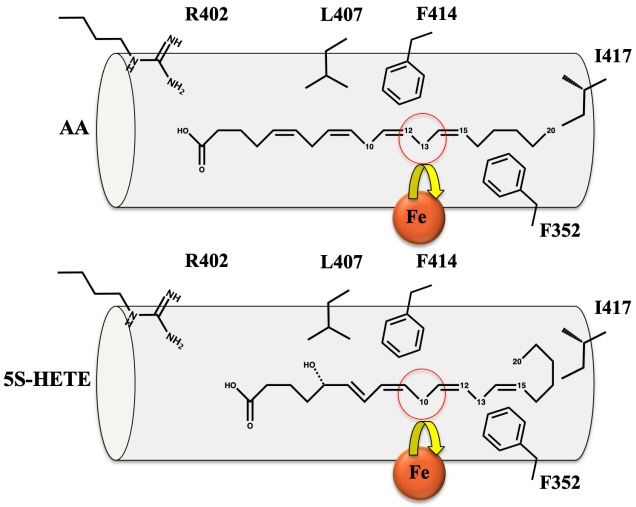

Figure 2. Model of the active site of h15-LOX-1, showing amino acid residues hypothesized to influence positional specificity with AA. The top figure depicts positioning of AA, while the bottom depicts positioning of 5S-HETE. h15-LOX-1 primarily abstracts a hydrogen from C13 of AA and C10 of 5S-HETE, which indicates that the two substrates must be positioned differently in the active site relative to the catalytic iron. The hydrogen bond between the alcohol of 5S-HETE and the carbonyl of I399 is not shown.

h15-LOX-1 primarily catalyzes the abstraction of the pro-S hydrogen from C13 of AA and C15 of DHA.[32] To explain the altered positional specificity of h15-LOX-1 with 5S-HETE, 5S-hydroxy-6E,8Z,11Z,14Z,17Z-eicosapentaenoic acid (5S-HEPE) and 7S-HDHA, h15-LOX-1 must primarily abstract from C10 of AA/EPA and C12 of DHA. This implies deeper insertion of the substrate into the active site cavity for these two oxylipins (**Figure 2**). Molecular modeling has indicated that the alcohol of 5S-HETE and 7S-HDHA forms a hydrogen bond with the backbone carbonyl of I399 which positions the oxylipin substrates deeper in the active site compared with AA and DHA[15, 17]. The proposed contribution of additional active site amino acids to substrate binding of 5S-HETE and 7S-HDHA indicates that the existing model of positional specificity in h15-LOX-1 may require additional refinement. The present study investigates whether the established residues which interact with AA also explain the structural basis for the altered positional specificity of h15-LOX-1 with 5S-HETE, 5S-HEPE, and 7S-HDHA

and which LOX isozyme could be involved in the biosynthetic pathway for the production of the SPM, RvE_4.

Experimental Procedures

Expression and Purification of h15-LOX-1 and h15-LOX-2.

Overexpression and purification of his-tagged wild-type and mutant h15-LOX-1 (Accession ID: P16050) and h15-LOX-2 (Accession ID: O15296) was performed using cation exchange and nickel-affinity chromatography as previously described[33, 34]. Overexpression and purification of wild-type h5-LOX was performed by ammonium-sulfate precipitation as previously described[35]. The purity of h15-LOX-1 and h15-LOX-2 were assessed by SDS gel to be greater than 85%, and metal content was assessed on a Finnigan inductively-coupled plasma-mass spectrometer (ICP-MS), via comparison with iron standard solution. Cobalt-EDTA was used as an internal standard. The concentration of h5-LOX (Accession ID: P09917) in the ammonium-sulfate was determined as described before,[15, 17] and due to the difficulty determining the iron content of crude ammonium sulfate-precipitated extracted enzyme, the metalation of h5-LOX was assumed to be 100%, indicating that the estimated kinetic parameters presented in this work are lower limits.

Site-directed Mutagenesis.

Amino acid numbering for h15-LOX-1 refers to the sequence with UniProt accession number P16050 without the 6XHis-tag and with the N-terminal methionine assigned as amino acid number one. The following mutations were introduced into h15-LOX-1: F352L, F352W, E398L, I399A, R402L, L407A, F414L, F414W, I417A, I417M, Q595L. Primers were designed using the Agilent Technologies (CA, USA) online primer-design tool found at: (***http://www.genomics.agilent.com/primerDesignProgram.jsp***) Mutations were introduced with a QuikChange®II site-directed mutagenesis kit from Agilent Technologies using the included protocol. The mutations were confirmed by sequencing the LOX insert in the pFastBac1 shuttle vector (Eurofins Genomics, KY, USA).

Production and isolation of Oxylipins from h5-LOX

7S-hydroperoxy-4Z,8E,10Z,13Z,16Z,19Z-docosahexaenoic acid (7S-HpDHA) was synthesized by reaction of DHA (25-50 μM) with h5-LOX. The reaction was carried

out for 2 hours in 800 mL of 25mM HEPES, pH 7.5 containing 50mM NaCl, 100 μM EDTA and 200 μM ATP. The reaction was quenched with 0.5% glacial acetic acid, extracted 3 times with 1/3 volume dichloromethane and evaporated to dryness under N2. The products purified isocratically via high performance liquid chromatography (HPLC) on a Higgins Haisil Semi-preparative (5μm, 250mm x 10mm) C18 column with 45:55 of 99.9% acetonitrile, 0.1% acetic acid and 99.9% water, 0.1% acetic acid. 7S-HDHA was synthesized as performed for 7S-HpDHA with trimethylphosphite added as a reductant prior to HPLC. The isolated products were assessed to be greater than 95% pure by LC-MS/MS. 5S-HpETE and 5S-hydroperoxy-6E,8Z,11Z,14Z,17Z-eicosapentaenoic acid (5S-HpEPE) were synthesized by reaction of AA and EPA, respectively, (25-50 μM) with h5-LOX. The reactions were carried out for 1 hour in 1000 mL of 25mM HEPES, pH 7.5 containing 50mM NaCl, 100 μM EDTA and 200 μM ATP. The reactions were quenched with 0.5% glacial acetic acid, extracted 3 times with 1/3 volume dichloromethane and evaporated to dryness under N_2. 5S-HETE and 5S-HEPE were synthesized as performed for 5S-HpETE and 5S-HpEPE with trimethylphosphite added as a reductant prior to HPLC. The products purified isocratically via high performance liquid chromatography (HPLC) on a Higgins Haisil Semi-preparative (5μm, 250mm x 10mm) C18 column with 45:55 of 99.9% acetonitrile, 0.1% acetic acid and 99.9% water, 0.1% acetic acid. The products were determined to be of the S configuration, as described previously.[15, 36]

Steady State Kinetics of h15-LOX-1

h15-LOX-1 steady-state kinetic reactions were constantly stirred at ambient temperature, in a 1 cm^2 quartz cuvette containing 2 mL of 25 mM HEPES, pH 7.5 with substrate, such as AA, DHA, 5S-HETE, 5S-HpETE, 7S-HDHA, or 7S-HpDHA. Substrate concentrations were varied from 0.25 μM to 10 μM for AA or 0.5 μM to 40 μM for 5S-HETE and 5S-HpETE. DHA concentrations were varied from 0.25-10 μM, 7S-HDHA concentrations were varied from 0.3-15 μM, and 7S-HpDHA concentrations were varied from 0.3-20 μM. Concentrations of AA and DHA were determined by measuring the amount of 15S-HpETE and 17S-hydroperoxy-4Z,7Z,10Z,13Z,15E,19Z-docosahexaenoic acid (17S-HpDHA), respectively, produced from complete reaction with soybean lipoxygenase-1 (sLO-1). Concentrations of 5S-HETE, 5S-HpETE, 7S-HDHA, and 7S-HpDHA were determined by measuring the absorbance at 234 nm.

Reactions were initiated by the addition of h15-LOX-1 (~200-600 nM final concentration) and were monitored on a Perkin-Elmer Lambda 45 UV/VIS spectrophotometer. Product formation was determined by the increase in absorbance at 234 nm for 5S-HETE (ε_{234} = 27,000 M^{-1} cm^{-1}), 270 nm for 5S,12S-diHETE (ε_{270} = 40,000 M^{-1} cm^{-1}), 254 nm for 5S,15S-diHETE (ε_{254} = 21,500 M^{-1} cm^{-1})[37], 234 nm for 7S-HpDHA (ε_{234} = 25,000 M^{-1} cm^{-1}) and 270 nm for 7S,14S-diHDHA (ε_{270} = 40,000 M^{-1} cm^{-1})[38, 39]. 5S,15S-diHDHA and 7S,17S-diHDHA have an absorbance max of 245 nm, however, due to overlap with the substrate peak at 234 nm formation of this product was measured at 254 nm using an extinction coefficient of 21,500 M^{-1} cm^{-1} to adjust for the decreased rate of absorbance change at this peak shoulder[40]. KaleidaGraph (Synergy) was used to fit initial rates (at less than 20% turnover), as well as the second order derivatives (k_{cat}/K_M) to the Michaelis-Menten equation for the calculation of kinetic parameters.

Product Analysis of LOX reactions with AA, DHA, 5S-HETE, 5S-HEPE and 7S-HDHA

Reactions were carried out in 2 mL of 25 mM HEPES, pH 7.5 with stirring at ambient temperature. Reactions with AA and DHA contained 10 μM substrate and ~200 nM h15-LOX-1. Those with 5S-HETE, 5S-HEPE, 7S-HDHA and contained 20 μM substrate and ~550 nM h15-LOX-1, due to their low reactivity. Reactions were monitored via UV-vis spectrophotometer and quenched at 50% turnover with 0.5% glacial acetic acid. Each quenched reaction was extracted with 6 mL of DCM and reduced with trimethylphosphite. The samples were then evaporated under a stream of N_2 to dryness and reconstituted in 50 μL of methanol containing 3 μM 13-HODE as an internal standard. Control reactions without enzymes were also conducted and used for background subtraction, ensuring oxylipin degradation products were removed from analysis. Reactions were analyzed in the same manner mentioned above. MS was performed in a targeted manner with a mass list containing the following m/z ratios ± 0.5: 317.2 (HEPE), 319.2 (HETE), 333.2 (diHEPE), 335.2 (diHETE) 343.4 (HDHA), 359.4 (diHDHA). Products were identified by matching retention times, UV spectra, and fragmentation patterns to known standards, or in the cases where MS standards were not available, structures were deduced from comparison with known and theoretical fragments. A representative trace of the reaction of AA with h15-LOX-1 demonstrates

the relative purity of the oxylipin products and the negative control (Figure S1 in the Supporting Information).

Results and Discussion

The docking model proposed for AA binding in the active site of h15-LOX-1 postulates three regions of the active site to be important for determining the positional specificity which interact with the head, middle and base of the fatty acid (**Figure 3**). The key residues outlined in **Figure 3** are in h15-LOX-1 are R402, L407, F414, I417 and F352. To determine if 5S-HETE binds in a similar fashion to AA, we created a series of mutants to investigate the binding constraints of 5S-HETE and assayed their kinetic and product profiles.

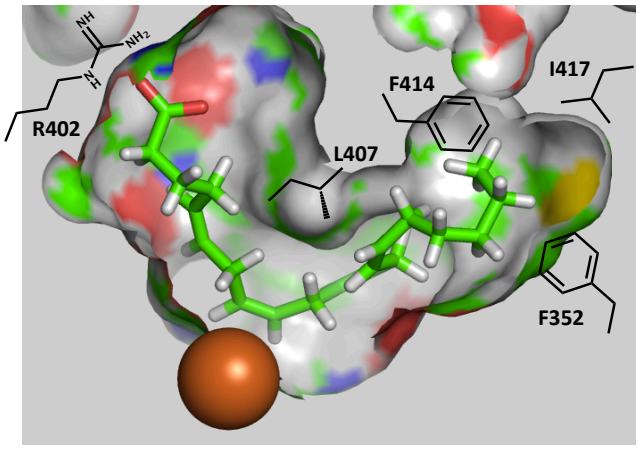

Figure 3. Model of the active site of h15-LOX-1 showing L-shaped binding cavity, position of catalytic iron in orange and AA in green at middle. Amino acids shown to play a role in positional specificity of AA are highlighted: R402, L407, F414, I417, F352.

Binding to substrate carboxylate: R402

Positively charged amino acids can play a role in binding the carboxylate of fatty acids[41]. R402, located near the entrance to the active site cavity, is conserved in both h12-LOX and h15-LOX-1 and is proposed to interact with the carboxylic acid moiety of AA[23]. This interaction is thought to stabilize the substrate fatty acid in the active site with

	AA			5S-HETE		
	K_M	k_{cat}	k_{cat}/K_M	K_M	k_{cat}	k_{cat}/K_M
wild-type	5.1 ±0.3	10 ±1	2.1 ±0.3	4.9 ±0.6	1.1 ±0.4	0.22 ±0.08
R402L	9.8 ±1.5	7.2 ±0.5	0.73 ±0.13	6.3 ±0.6	3.6 ±0.1	0.55 ±0.06

Table 1. Steady state kinetics of wild-type and R402L h15-LOX-1 with AA and 5S-HETE substrates. K_M is in units of μM, k_{cat} is in units of $sec^{-1}\mu M^{-1}$, k_{cat}/K_M is in units of $sec^{-1}\mu M^{-1}$.

the methyl end orientated towards the bottom of the active site pocket. To test whether this model can be applied to 5S-HETE, R402 was replaced with leucine in h15-LOX-1. However, only marginal change was observed in the steady-state Michaelis-Menten kinetics of 5S-HETE with R402L compared with the wild-type enzyme (**Table 1**). While this mutation slightly lowered the kinetic parameters for AA, it is observed that the k_{cat} is approximately 3-fold greater for R402L over that of wild-type with 5S-HETE as the substrate, which is unexpected. Considering that Arg is larger than Leu, it is possible that the smaller Leu allows for a more rapid product release of the larger 5S-HETE. The product profile showed that the percentage of 5S-HETE oxygenated by R402L at C12 did not change (within error). In total, the data indicate that R402L does not significantly impact 5S-HETE catalysis or positioning, relative to AA (**Table 2**). It should be noted that in the current work, the product profile of our R402L mutant with AA was similar to previously published work[23], however the kinetic parameters of R402L were not. The mutant, R402L, demonstrated a comparable k_{cat} with AA to that of the wild-type enzyme, however the k_{cat}/K_M was only 3-fold lower that wild-type (**Table 1**), which is smaller than the 7-fold change seen previously[23]. This smaller change is consistent with recent studies on h12-LOX, which demonstrated negligible kinetic effects with the R402L mutant[11]. The smaller kinetic effect for R402L than previously reported could be due to differences in the experimental design. The prior kinetic work used 13-HpODE, a known allosteric effector[42], detergents and high concentrations of fatty acid substrate. These conditions could lead to substrate inhibition and hence affect the kinetic parameters.

	AA		5S-HETE	
	% C15	**% C12**	**% C15**	**% C12**
wild-type	85 ±4	15 ±4	14 ±6	86 ±6
R402L	73 ±6	27 ±6	8 ±2	92 ±2

Table 2. Product profile of wild-type and R402L h15-LOX-1 with AA and 5S-HETE. The percent of the carbon which is being oxidized is presented (i.e., %C15 is percent oxidation on C15 of the substrate).

Narrow midpoint of active site cavity: L407

L546 is thought to define the bend point of the L-shaped active site cavity of soybean 15-LOX (s15-LOX), based on docking of AA into the crystal structure of s15-LOX[23, 43]. Sequence alignment shows that this leucine is conserved in the majority of

	AA			5S-HETE		
	K_M	k_{cat}	k_{cat}/K_M	K_M	k_{cat}	k_{cat}/K_M
wild-type	5.1 ±0.3	10 ±1	2.1 ±0.3	4.9 ± 0.6	1.1 ±0.4	0.22 ±0.08
L407A	4.9 ±1.2	2.0 ±0.4	0.41 ±0.08	7.9 ± 1.4	0.7 ±0.1	0.09 ±0.02

Table 3. Steady state kinetics of wild-type and L407A h15-LOX-1 with AA and 5S-HETE. K_M is in units of μM, k_{cat} is in units of $sec^{-1}\mu M^{-1}$, k_{cat}/K_M is in units of $sec^{-1}\mu M^{-1}$.

lipoxygenases and is homologous to L407 in humans[23]. Substituting a smaller amino acid at this location in h12-LOX resulted in a loss of activity and a shift to greater oxygenation at C15, by widening the active site across from the catalytic iron[11]. To test whether L407 influences the positioning of AA or 5S-HETE within the active site, L407A was generated. For AA, the k_{cat} and k_{cat}/K_M values decreased approximately 5-fold compared to wild-type, but for 5S-HETE, the values decreased even less (**Table 3**). The greater decrease in kinetic values for AA than that of 5S-HETE possibly suggests that the larger 5S-OH of 5S-HETE is filling the missing space of the L407A mutant, thus diminishing the mutational effect. When reacting with AA and 5S-HETE, L407A produces more C12 products with AA than wild-type, but similar product ratios for 5S-HETE (**Table 4**). These product profile data are similar to the kinetic data in that L407A affects the positioning of AA more than that of 5S-HETE, supporting the hypothesis that the larger 5S-HETE is better positioned for catalysis in the L407A active site.

	AA		5S-HETE	
	% C15	**% C12**	**% C15**	**% C12**
wild-type	85 ±4	15 ±4	14 ±6	86 ±6
L407A	67 ±7	33 ±7	9 ±2	91 ±2

Table 4. Product profiling of wild-type and L407A h15-LOX-1 with AA and 5S-HETE. The percent of the carbon which is being oxidized is presented (i.e., %C15 is percent oxidation on C15 of the substrate).

Π-stacking interactions with substrate double bonds: F414

It has previously been determined that the Δ11 double bond of AA is positioned in the active site of h15-LOX-1 to form π–π stacking interactions with F414[23]. This interaction is also observed in h12-LOX with F414, and could be considered a common structural feature in hLOX biochemistry[11]. To test whether F414 of h15-LOX-1 would also interact with 5S-HETE, the catalysis and product profile was investigated. Both the k_{cat} and k_{cat}/K_M values for F414I with 5S-HETE decreased over 15-fold compared to wild-type (**Table 5**), but the products generated from the reaction with 5S-HETE showed no change relative to wild-type (**Table 6**). Mutation of this residue to tryptophan, F414W,

	AA			5S-HETE		
	K_M	k_{cat}	k_{cat}/K_M	K_M	k_{cat}	k_{cat}/K_M
Wild-type	5.1 ±0.3	10 ±1	2.1 ±0.3	4.9 ± 0.6	1.1 ±0.4	0.22 ±0.08
F414I	6.6 ±0.9	1.2 ± 0.4	0.18 ±0.03	4.7 ± 0.7	0.073 ± 0.03	0.013 ± 0.006
F414W	6.8 ±0.5	12 ±1	1.8 ±0.1	4.2 ± 0.6	0.95 ± 0.4	0.23 ± 0.09

Table 5. Steady state kinetics of wild-type, F414I and F414W h15-LOX-1 with AA and 5S-HETE. K_M is in units of μM, k_{cat} is in units of $sec^{-1}\mu M^{-1}$, k_{cat}/K_M is in units of $sec^{-1}\mu M^{-1}$.

restored the wild-type activity of the enzyme for 5S-HETE, with both k_{cat} and k_{cat}/K_M nearly returning to their wild-type values. The recovery of activity with the addition of the aromatic tryptophan for the catalysis of 5S-HETE is similar to what was seen

	AA		5S-HETE	
	% C15	% C12	% C15	% C12
Wild-type	85 ± 4	15 ± 4	14 ± 6	86 ± 6
F414I	82 ± 2	18 ± 2	12 ± 2	88 ± 2
F414W	95 ± 1	5 ± 1	32 ± 2	68 ± 2

Table 6. Product profiling of wild-type, F414I and F414W h15-LOX-1 with AA and 5S-HETE. The percent of the carbon which is being oxidized is presented (i.e., %C15 is percent oxidation on C15 of the substrate).

previously with AA and indicates that there are also π–π stacking interactions between 5S-HETE and F414. For comparison, we confirmed the previously established interaction of F414 and AA (**Table 5**)[23]. Interestingly, F414W caused more oxygenation to occur at C15 for both AA and 5S-HETE. This is consistent with the "dip-stick" substrate binding model where the larger tryptophan prohibits the deeper entry of the substrate, relative to phenylalanine, and thus increases the production of the 15-product.

Depth of the of active site cavity: I417 and F352

Previous work indicated that F353 contributed to the positional specificity in s15-LOX by affecting the depth of the active site[44]. This hypothesis was extended to the sequence equivalent residue in h15-LOX-1 with work on chimeric mutants, which showed a similar role for F352[27]. I417 has also been implicated in binding the methyl end of the substrate because of its position at the bottom of the active site in h12-LOX[11, 45] and h15-LOX-1[24]. Decreasing the residue size of either F352 or I417 in h15-LOX-1 increases the cavity size and thus increases oxygenation at C12 due to AA positioning deeper in the

	AA			5S-HETE		
	K_M	k_{cat}	k_{cat}/K_M	K_M	k_{cat}	k_{cat}/K_M
wild-type	5.1 ±0.3	10 ±1	2.1 ±0.3	4.9 ±0.6	1.1 ±0.4	0.22 ±0.08
I417A	3.9 ±1.5	5.1 ±1.8	1.3 ±0.5	3.7 ±1.5	0.5 ±0.2	0.14 ±0.06
I417M	1.9 ±0.3	8.0 ±0.5	4.2 ±0.4	3.5 ±0.4	3.8 ±0.2	1.1 ±0.2
F352L	4.3 ±2	8.4 ±3	1.9 ±0.8	4.4 ±2	0.91 ±0.3	0.21 ±0.08
F352W	3.5 ±0.9	11 ±1	3.1 ±0.6	20 ±5	1.3 ±0.2	0.065 ±0.01

Table 7. Steady state kinetics of wild-type and various mutants of h15-LOX-1 with AA and 5S-HETE. K_M is in units of μM, k_{cat} is in units of $sec^{-1}\mu M^{-1}$, k_{cat}/K_M is in units of $sec^{-1}\mu M^{-1}$.

active site, as seen in previous work[10]. To extend this work and determine if the active site depth influences the reactivity of 5S-HETE, kinetics were investigated with smaller amino acids at positions 352 and 417. Compared to wild-type, the k_{cat} and k_{cat}/K_M values for I417A and F352L with both AA and 5S-HETE were approximately the same as wild-type (**Table 7**). This is remarkable considering that the oxygenation of AA at C12 increases dramatically for both I417A and F352L (**Table 8**), indicating a shift in the positioning of AA deeper in the active site pocket due to the smaller active site residues, but only a small change in rate is observed. With respect to 5S-HETE, oxygenation of C12 is already the major product, thus enlarging the active site has only a slight change in both the kinetics and product profile because 5S-HETE is already positioned deep in the active site.

	AA		5S-HETE	
	% C15	% C12	% C15	% C12
wild-type	85 ± 4	15 ± 4	14 ± 6	86 ± 6
I417A	22 ± 2	71 ± 2	3 ± 1	97 ± 1
I417M	87 ± 2	13 ± 2	16 ± 2	84 ± 2
F352L	16 ± 3	81 ± 3	5 ± 2	95 ± 2
F352W	96 ± 2	4 ± 2	69 ± 6	31 ± 6

Table 8. Product profiling of wild-type and various mutants of h15-LOX-1 with AA and 5S-HETE. The percent of the carbon which is being oxidized is presented (i.e., %C15 is percent oxidation on C15 of the substrate, i.e. AA and 5S-HETE).

With the smaller residues at 417 and 352 allowing the substrate to bind deeper into the active site, it was hypothesized that larger residues near the bottom of the active site would have the opposite effect by restricting substrate binding and thereby shifting positional specificity from C12 to C15. For I417M, the product profile for both AA and 5S-HETE were unchanged relative to wild-type, indicating that the positioning of the two substrates has not changed significantly with this mutant (**Table 8**, **Figure 4**). Interestingly, the kinetic values for both AA and 5S-HETE increase with I417M. Considering that the product profiles for both of these substrates is similar to that of wild-type enzyme, it is difficult to explain this result by sterics, so possibly the active site dynamics are affected.

For F352W, the percent of C15 product increased for both AA and 5S-HETE relative to wild-type and I417M, indicating that F352W has a greater decrease in active site volume (**Table 8**, **Figure 5**). The effect of F352W is larger for 5S-HETE than that of AA, with the C15 percent increasing from 14% to 69%, possibly indicating that 5S-HETE binds deeper into the pocket than AA and thus the reduced active site volume has a larger effect. The kinetic data reflect this hypothesis with the k_{cat}/K_M of 5S-HETE decreasing 3-fold, while the value for AA increases 1.5-fold, indicating a larger change in 5S-HETE positioning in the active site that that of AA (**Table 7)**.

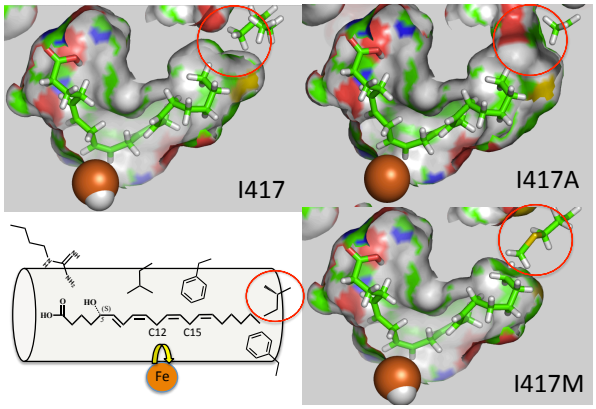

Figure 4. Model of the active site of h15-LOX-1 showing position of I417 and the effects that various amino acid mutations have on the size of the active site. I417A creates more space at the bottom of the active site, while I417M creates less space.

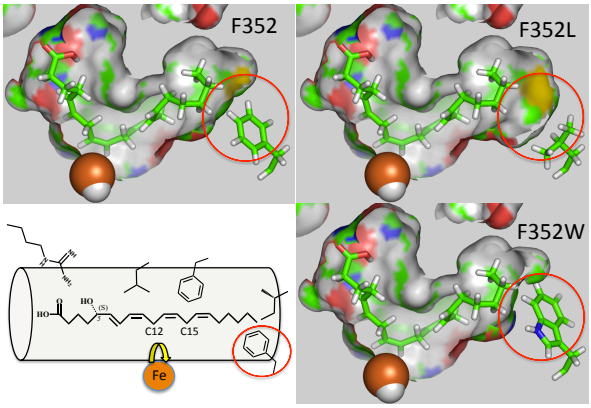

Figure 5. Model of the active site of h15-LOX-1 showing position of F352 and the effects that various amino acid mutations have on the size of the active site. F352L creates more space at the bottom of the active site, while F352W creates less space.

Depth of active site with DHA and 7S-HDHA

The dip-stick model of substrate binding by h15-LOX-1 posits that the depth of the active site is a primary determinant for how far the methyl end of a substrate can insert. For 5S-HETE, its position in the active site of h15-LOX-1 is deeper than that of AA and thus the 5S,12S-diHETE product is primarily synthesized. 7S-HDHA shows an analogous change in positional specificity, with h15-LOX-1 producing the non-canonical product, 7S,14S-diHDHA, instead of 7S,17S-diHDHA[17]. 7S-HDHA and 5S-HETE are structurally similar in that the C7 and C5 alcohols are both located on the ω-16 carbon relative to the methyl end of the substrate and h15-LOX-1 oxygenates at their ω-9

positions, C14 and C12, respectively. Since h15-LOX-1 shows similar shifts in product profile with both 7S-HDHA and 5S-HETE, it is likely that they are bound in the active site in a similar fashion[15, 17]. Consequently, it is likely that amino acid mutations changing the depth of the active site cavity will affect 7S-HDHA similarly to that of 5S-HETE.

To investigate this hypothesis, the positional specificity of h15-LOX-1 with both DHA and 7S-HDHA were assayed with I417A, I417M, F352L and F352W. h15-LOX-1 reacting with DHA produced a mixture of primarily the 14- and 17-oxylipins, as see previously (**Table 9**).[46] When reacting with I417A, DHA displayed the expected shift to more oxygenation at C14 and less oxygenation at C17 relative to wt 12-LOX, as the

	DHA				7S-HDHA			
	% C20	% C17	% C14	% C11	% C20	% C17	% C14	% C11
wild-type	6 ±2	65 ±4	22 ±5	6 ±1	-	10 ±6	90 ±6	0
I417A	2 ±2	55 ±8	40 ±8	2 ±2	-	-	97 ±1	3 ±1
I417M	2 ±1	73 ±2	24 ±1	-	-	36 ±2	64 ±2	-
F352L	29 ±3	47 ±3	23 ±3	-	-	-	100	-
F352W	7 ±2	79 ±6	10 ±3	-	-	94 ±1	6 ±1	-

Table 9. Product profiling of wild-type and various mutants of h15-LOX-1 with DHA and 7S-HDHA. The percent of the carbon which is being oxidized is presented (i.e., %C11 is percent oxidation on C11 of the substrate). K_M is in units of μM, k_{cat} is in units of $sec^{-1}\mu M^{-1}$, k_{cat}/K_M is in units of $sec^{-1}\mu M^{-1}$.

substrate was able to position deeper in the active site relative to the iron (**Table 9**.) The reaction of DHA with I417M demonstrated a small shift to increased oxygenation at C17, resulting from the slightly bulkier methionine residue. The reaction between F352L and DHA showed the expected decrease in oxygenation at C17, however instead of an increase at C14, a large increase in oxygenation at C20 occurred. It is unclear why this product increased, but it may indicate a change in the overall substrate orientation due to folding of the substrate methyl end so that it is positioned less deep in the active site. When reacting with DHA, F352W produced 79% of the 17-product, compared to 65% with wild-type, demonstrating that the bulkier tryptophan substitution produces the largest shift in product profile, similar to the results with AA (**Table 8**).

The product profile with 7S-HDHA as the substrate shows similar results as that with DHA as the substrate, with smaller substitutions allowing for deeper entry of 7S-HDHA into the active site (**Table 9**). The smaller amino acids of F352L and I417A both

increase the amount of oxygenation occurring on C17, from 90% in wild-type to 97% with I417A and 100% with F352L. Substituting larger amino acids in these positions had the expected opposite effect. The reaction with I417M decreased oxygenation at C17 from 90% in wild-type to 64 % in the mutant. The reaction of F352W decreased oxygenation at C17 to only 6%, a near complete reversal of the altered positional specificity seen with 7S-HDHA and the wild-type enzyme.

When comparing the product profile of 5S-HETE (**Table 8**) and 7S-HDHA (**Table 9**), I417M has a much larger effect on 7S-HDHA, which may indicate that the larger size of 7S-HDHA compared with 5S-HETE, makes it more sensitive to the small change in active site depth brought about by I417M. In total, these data indicate that the shift in positional specificity is related to the size of the amino acids at the bottom of the active site for 7S-HDHA, consistent with the results obtained for 5S-HETE and indicates a similar mode of binding between 5S-HETE and 7S-HDHA.

Coordination of alcohol group of 5S-HETE/7S-HDHA through hydrogen bonding with the carbonyl backbone of I399

Molecular dynamic simulations coupled with computational docking revealed a possible intermolecular bond in the active site of h15-LOX-1 with the hydroxyl group of 5S-HETE/7S-HDHA[15, 17]. The interaction observed was a hydrogen bond with the backbone carbonyl of I399. The positioning of this carbonyl hydrogen bond in the active site, relative to the coordinating iron and oxygen channel, is proposed to hold the substrate in a manner that makes enzymatic hydrogen abstraction more likely at the ω-9 carbon than the ω-6 carbon. To test this hypothesis, the I399A mutant was reacted with 5S-HETE, with the hope that the side chain would affect the hydrogen bond to the backbone carbonyl, however, the reactivity and product profile of I399A were comparable to that of wild-type (data not shown). This is an inconclusive result and we

	EPA		**5S-HEPE**	
	% C15	**% C12**	**% C15**	**% C12**
h15-LOX-1	87 ± 2	13 ± 2	22 ± 1	78 ± 1
h15-LOX-2	100	0	93± 3	7 ± 3

Table 10. In vitro Product profile of h15-LOX-1 and h15-LOX-2 reacting with EPA and 5S-HEPE. The percent of the carbon which is being oxidized is presented (i.e., %C15 is percent oxidation on C15 of the substrate).

are currently pursuing another line of inquiry in order to determine the structural requirements for the non-canonical activity of h15-LOX-1.

***In Vitro* Biosynthesis of Resolvin E_4 (5S,15S-diHEPE)**

Previous work has proposed that the biosynthesis of RvE_4 is accomplished by h15-LOX-1 reacting with EPA to produce 15S-HpEPE, which is then further oxidized by h5-LOX to yield the 5S,15S-diHEPE product (RvE_4)[18]. However, past *in vitro* experiments have shown ω-6 oxylipins to be extremely poor substrates for h5-LOX[15, 17], which raises questions regarding the proposed biosynthetic pathway of RvE_4. To investigate this further, *in vitro* reactions with h15-LOX-1 and h15-LOX-2 in the presence of 5S-HEPE were carried out. Product profile analysis of the h15-LOX-1 products revealed a shift in positional specificity, similar to that seen with the other ω-6 oxylipins, with more 5S,12S-diHEPE being generated than 5S,15S-diHEPE, 78% and 22%, respectively (**Table 10**). However, h15-LOX-2 produced mostly 5S,15S-diHEPE (93%, **Table 10**), supporting our previous work that h15-LOX-2 primarily generates the 5S,15S dioxylipin product and, thus, may be the primary source of RvE_4. This was previously observed by Kutzner et al. when h5-LOX and h15-LOX-2 were added to a buffer containing EPA.[16]

Regarding the relative rates of catalysis for RvE_4, 5S-HEPE (10 μM) was reacted with h15-LOX-2 and 15S-HEPE (10 μM) with h5-LOX (**Table 11**). The data indicates that h15-LOX-2 is a 40-fold faster catalyst than h5-LOX when reacting with their secondary substrates, although they have comparable rates with AA and EPA as substrates, at 10 μM. Given the relative kinetic capabilities of h5-LOX with 15S-HETE and h15-LOX-2 with 5S-HETE[15, 17, 47, 48], h15-LOX-2 appears to be the faster catalyst for the final step in RvE_4 generation. However, considering that in vivo, the level of substrate could be lower than 10 μM and that the cell contains 5-LOX activating protein (FLAP)

and other cellular components, we cannot discount a change in relative LOX isozyme reactivity due to the cellular milieu.

Enzyme	Substrate	V_{max} (mol/sec^{-1}/mol^{-1})
h5-LOX*	AA	0.15 ± 0.03
h5-LOX*	EPA	0.14 ± 0.01
h5-LOX*	15S-HEPE	0.0037 ± 0.0006
h15-LOX-2	AA	0.24 ± 0.04
h15-LOX-2	EPA	0.26 ± 0.03
h15-LOX-2	5S-HEPE	0.17 ± 0.03

Table 11. V_{max} comparison of h5-LOX and h15-LOX-2 with secondary substrates. *The ammonium sulfate-precipitated h5-LOX protein concentration was estimated from SDS-PAGE as previously published (Perry et al., 2020), such that protein concentrations between the LOXs was maintained.

Conclusions

The fatty acid docking mode developed to explain the positional specificity of h15-LOX-1 (ALOX15) reactivity with AA[23] includes 5 principle residues: R402, L407, F414, I417 and F352. Of these five, three are conserved in the mouse ortholog, ALOX15 (residues 402, 407, 414, 69% identity to human ALOX15) but only two are conserved in h15-LOX-2 (ALOX15B, residues 352, 407, 38% identity to human ALOX15). These results are intriguing since the gene sequence of mouse ALOX15 is more similar to human ALOX15, but it primarily produces 12-HETE. However, the gene sequence of human ALOX15B is less similar to human ALOX15, but it primarily produces 15-HETE. These data illustrate the observation that the sequence similarity between genes is not as important as specific residues in the active site.

In the current work, the established AA docking model for h15-LOX-1 only partially explains the altered positional specificity of h15-LOX-1 with 5S-HETE and 7S-HDHA. R402L did not have a large effect on 5S-HETE catalysis, indicating that this interaction with the substrate carboxylate is not important for 5S-HETE positioning, as previously seen for h12-LOX and AA[11]. F414 appears to π–π stack with 5S-HETE, as seen with AA binding, indicating an interaction between a double bond of 5S-HETE and F414. Further evidence of the importance of steric interactions at the bottom of the active site cavity comes from mutagenesis of F352 and I417, which plays the largest roles in 5S-

HETE positioning. Decreasing the size of the amino acids in these locations shifted oxygenation of 5S-HETE to C12, while increasing the size of these residues reversed the positional specificity of h15-LOX-1 with 5S-HETE to C15, with F352 having a larger impact than I417. Mutants at these locations demonstrated a similar effect with 7S-HDHA, indicating that both substrates interact with the bottom of the active site. Together, these data indicate that of the three regions proposed to control positional specificity of h15-LOX-1, π–π stacking and active site cavity depth are the primary determinants of positional specificity with 5S-HETE and 7S-HDHA, similar to what was observed with AA as the substrate. Mutation of I399 did not support our hypothesis that its carbonyl backbone hydrogen bonded with the ω-16 alcohol. However, we have recently determined that unsaturation and length of the oxylipin substrate affects the product profile, undermining our I399 carbonyl hypothesis. We are currently investigating this line of inquiry to identify the structural property which accounts for the non-canonical product profile of h15-LOX-1. Furthermore, experimentation by Saam et al.[49] with murine 12/15 lipoxygenase and Klinman and coworkers [50, 51] with soybean 15-lipoxygenase has provided compelling evidence for the presence of a dynamic oxygen channel linking the enzyme surface to the active site of lipoxygenases. The change in positional specificity of h15-LOX-1 when reacting with 5S-HETE and 7S-HDHA could also be affected by changes in the oxygen channel with oxylipin binding, which we are currently investigating.

Finally, the altered reactivity of h15-LOX-1 with 5S-HEPE suggests that the biosynthesis of RvE_4 may not proceed through h15-LOX-1. The above *in vitro* reaction rates and product profiles suggest that the biosynthetic pathway for RvE_4 production could be initiated with h5-LOX biosynthesizing 5S-HEPE from EPA, followed by h15-LOX-2 producing 5S,15S-diHEPE (i.e., RvE_4). It should be mentioned that 5,15-oxylipin has been observed in a variety of human cell lines,[52, 53] indicating important roles for h5-LOX and h15-LOX, but the order of biosynthetic steps and the specific identity of the h15-LOX isozyme remains unclear. Recently, Mainka et al. demonstrated that 5,15-oxylipin production was a primary product when 15-oxylipin was given to polymorphonuclear leukocytes (PMNL) and that h5-LOX was involved, with the presence of FLAP being critical.[54] Therefore, it could be that the lowered *in vitro* activity

of h5-LOX observed in our work is due to the dis-similar environment relative to the cellular milieu. However, the role of h15-LOX-1 remains unclear. Due to the cellular mixture of the PMNLs, Mainka et al. could not identify if h15-LOX-1 or h15-LOX-2 were the active partner in the biosynthesis of the 5,15-oxylipin, adding further obscurity to their biosynthetic pathway. Therefore, we are currently investigating the expression levels of the LOX isoforms in immune cells and their inhibition by specific LOX inhibitors during the inflammatory response to determine which LOX is involved in the production of RvE_4 and the order of the biosynthetic steps.

TOC Graphic

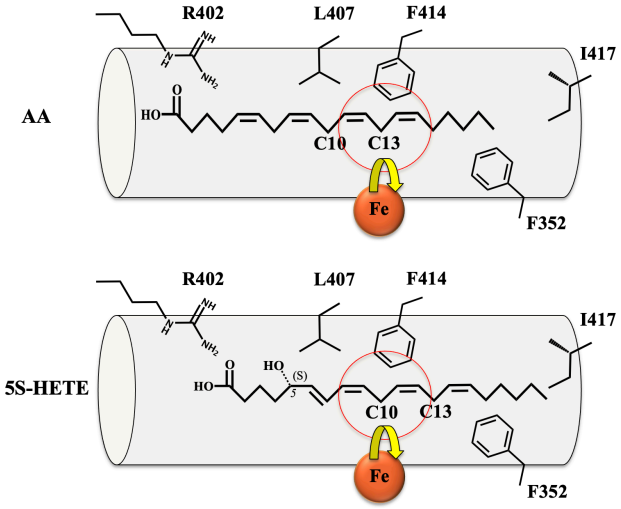
R402
L407
F414
I417
AA
HO
O
C10
C13
Fe
F352
R402
L407
F414
I417
5S-HETE
HO
O
HO
(S)
5
C10
C13
Fe
F352

References

[1] Brash, A. R. (1999) Lipoxygenases: Occurrence, Functions, Catalysis and Acquisition of Substrate, *J. Biol. Chem. 274*, 23679-23682.

[2] Kuhn, H., Saam, J., Eibach, S., Holzhutter, H. G., Ivanov, I., and Walther, M. (2005) Structural biology of mammalian lipoxygenases: enzymatic consequences of targeted alterations of the protein structure, *Biochem Biophys Res Commun 338*, 93-101.

[3] Mashima, K., Suzuki, S., Mori, T., Shimizu, T., Yamada, S., Hirose, S., Okamoto, S., and Suzuki, N. (2015) Chronic lymphocytic inflammation with pontine perivascular enhancement responsive to steroids (CLIPPERS) after treatment for Hodgkin's lymphoma, *Int J Hematol 102*, 709-712.

[4] Funk, C. D. (2006) Lipoxygenase pathways as mediators of early inflammatory events in atherosclerosis, *Arteriosclerosis, thrombosis, and vascular biology 26*, 1204-1206.

[5] Serhan, C. N. (2007) Resolution phase of inflammation: novel endogenous anti-inflammatory and proresolving lipid mediators and pathways, *Annual review of immunology 25*, 101-137.

[6] Serhan, C. N. (2010) Novel lipid mediators and resolution mechanisms in acute inflammation: to resolve or not?, *Am J Pathol 177*, 1576-1591.

[7] Wisastra, R., and Dekker, F. J. (2014) Inflammation, Cancer and Oxidative Lipoxygenase Activity are Intimately Linked, *Cancers (Basel) 6*, 1500-1521.

[8] Fabre, J. E., Goulet, J. L., Riche, E., Nguyen, M., Coggins, K., Offenbacher, S., and Koller, B. H. (2002) Transcellular biosynthesis contributes to the production of leukotrienes during inflammatory responses in vivo, *J Clin Invest 109*, 1373-1380.

[9] Brash, A. R., Boeglin, W. E., and Chang, M. S. (1997) Discovery of a second 15S-lipoxygenase in humans, *Proc Natl Acad Sci U S A 94*, 6148-6152.

[10] Sloane, D., Leung, R., Craik, C., and Sigal, E. (1991) A Primary Determinant for Lipoxygenase Positional Specificity, *Nature 354*, 149-152.

[11] Aleem, A. M., Tsai, W. C., Tena, J., Alvarez, G., Deschamps, J., Kalyanaraman, C., Jacobson, M. P., and Holman, T. (2019) Probing the Electrostatic and Steric Requirements for Substrate Binding in Human Platelet-Type 12-Lipoxygenase, *Biochemistry 58*, 848-857.

[12] Kuhn, H., Banthiya, S., and van Leyen, K. (2015) Mammalian lipoxygenases and their biological relevance, *Biochim Biophys Acta 1851*, 308-330.

[13] Bryant, R. W., Bailey, J. M., Schewe, T., and Rapoport, S. M. (1982) Positional specificity of a reticulocyte lipoxygenase. Conversion of arachidonic acid to 15-S-hydroperoxy-eicosatetraenoic acid, *J Biol Chem 257*, 6050-6055.

[14] Kuhn, H., Wiesner, R., Schewe, T., and Rapoport, S. M. (1983) Reticulocyte lipoxygenase exhibits both n-6 and n-9 activities, *Febs Lett 153*, 353-356.

[15] Perry, S. C., Horn, T., Tourdot, B. E., Yamaguchi, A., Kalyanaraman, C., Conrad, W. S., Akinkugbe, O., Holinstat, M., Jacobson, M. P., and Holman, T. R. (2020) Role of Human 15-Lipoxygenase-2 in the Biosynthesis of the Lipoxin Intermediate, 5S,15S-diHpETE, Implicated with the Altered Positional Specificity of Human 15-Lipoxygenase-1, *Biochemistry 59*, 4118-4130.

[16] Kutzner, L., Goloshchapova, K., Rund, K. M., Jubermann, M., Blum, M., Rothe, M., Kirsch, S. F., Schunck, W. H., Kuhn, H., and Schebb, N. H. (2020) Human lipoxygenase isoforms form complex patterns of double and triple oxygenated compounds from eicosapentaenoic acid, *Biochim Biophys Acta Mol Cell Biol Lipids 1865*, 158806.
[17] Perry, S. C., Kalyanaraman, C., Tourdot, B. E., Conrad, W. S., Akinkugbe, O., Freedman, J. C., Holinstat, M., Jacobson, M. P., and Holman, T. R. (2020) 15-Lipoxygenase-1 biosynthesis of 7S,14S-diHDHA implicates 15-lipoxygenase-2 in biosynthesis of resolvin D5, *J Lipid Res 61*, 1087-1103.
[18] Libreros, S., Shay, A. E., Nshimiyimana, R., Fichtner, D., Martin, M. J., Wourms, N., and Serhan, C. N. (2020) A New E-Series Resolvin: RvE4 Stereochemistry and Function in Efferocytosis of Inflammation-Resolution, *Front Immunol 11*, 631319.
[19] Hong, S., Gronert, K., Devchand, P. R., Moussignac, R. L., and Serhan, C. N. (2003) Novel docosatrienes and 17S-resolvins generated from docosahexaenoic acid in murine brain, human blood, and glial cells. Autacoids in anti-inflammation, *J Biol Chem 278*, 14677-14687.
[20] Green, F. A. (1990) Transformations of 5-HETE by activated keratinocyte 15-lipoxygenase and the activation mechanism, *Lipids 25*, 618-623.
[21] Green, A. R., Barbour, S., Horn, T., Carlos, J., Raskatov, J. A., and Holman, T. R. (2016) Strict Regiospecificity of Human Epithelial 15-Lipoxygenase-2 Delineates Its Transcellular Synthesis Potential, *Biochemistry 55*, 2832-2840.
[22] Ivanov, I., Kuhn, H., and Heydeck, D. (2015) Structural and functional biology of arachidonic acid 15-lipoxygenase-1 (ALOX15), *Gene 573*, 1-32.
[23] Gan, Q.-F., Browner, M. F., Sloane, D. L., and Sigal, E. (1996) Defining the arachidonic acid binding site of human 15-lipoxygenase, *J. Biol. Chem. 271*, 25412 - 25418.
[24] Sloane, D., Leung, R., Barnett, J., Craik, C., and Sigal, E. (1995) Conversion of Human 15-Lipoxygenase to an Efficient 12-Lipoxygenase - The Side-Chain Geometry of Amino Acids 417 and 418 Determine Positional Specificity, *Prot Eng 8*, 275-282.
[25] Sloane, D. L., Leung, R., Barnett, J., Craik, C. S., and Sigal, E. (1995) Conversion of Human 15-Lipoxygenase to an Efficient 12-Lipoxygenase - The Side-Chain Geometry of Amino Acids 417 and 418 Determine Positional Specificity, *Prot. Eng. 8*, 275-282.
[26] Sloane, D. L., and Sigal, E. (1994) On the positional specificity of 15-lipoxygenase, *Ann N Y Acad Sci 744*, 99-106.
[27] Borngraber, S., Kuban, R. J., Anton, M., and Kuhn, H. (1996) Phenylalanine 353 is a primary determinant for the positional specificity of mammalian 15-lipoxygenases, *J Mol Biol 264*, 1145-1153.
[28] Borngraber, S., Browner, M., Gillmor, S., Gerth, C., Anton, M., Fletterick, R., and Kuhn, H. (1999) Shape and specificity in mammalian 15-lipoxygenase active site - The functional, interplay of sequence determinants for the reaction specificity, *J. Biol. Chem. 274*, 37345-37350.
[29] Kuhn, H. (2000) Structural basis for the positional specificity of lipoxygenases, *Prostaglandins & other lipid mediators 62*, 255-270.

[30] Walther, M., Ivanov, I., Myagkova, G., and Kuhn, H. (2001) Alterations of lipoxygenase specificity by targeted substrate modification and site-directed mutagenesis, *Chem Biol 8*, 779-790.
[31] Vogel, R., Jansen, C., Roffeis, J., Reddanna, P., Forsell, P., Claesson, H. E., Kuhn, H., and Walther, M. (2010) Applicability of the triad concept for the positional specificity of mammalian lipoxygenases, *J Biol Chem 285*, 5369-5376.
[32] Snodgrass, R. G., and Brune, B. (2019) Regulation and Functions of 15-Lipoxygenases in Human Macrophages, *Front Pharmacol 10*, 719.
[33] Vasquez-Martinez, Y., Ohri, R. V., Kenyon, V., Holman, T. R., and Sepulveda-Boza, S. (2007) Structure-activity relationship studies of flavonoids as potent inhibitors of human platelet 12-hLO, reticulocyte 15-hLO-1, and prostate epithelial 15-hLO-2, *Bioorganic & Medicinal Chemistry 15*, 7408-7425.
[34] Amagata, T., Whitman, S., Johnson, T. A., Stessman, C. C., Loo, C. P., Lobkovsky, E., Clardy, J., Crews, P., and Holman, T. R. (2003) Exploring sponge-derived terpenoids for their potency and selectivity against 12-human, 15-human, and 15-soybean lipoxygenases, *J Nat Prod 66*, 230-235.
[35] Robinson, S. J., Hoobler, E. K., Riener, M., Loveridge, S. T., Tenney, K., Valeriote, F. A., Holman, T. R., and Crews, P. (2009) Using enzyme assays to evaluate the structure and bioactivity of sponge-derived meroterpenes, *Journal of Natural Products 72*, 1857-1863.
[36] Perry, S. C., Kalyanaraman, C., Tourdot, B. E., Conrad, W. S., Akinkugbe, O., Freedman, J. C., Holinstat, M., Jacobson, M. P., and Holman, T. R. (2020) 15-Lipoxygenase-1 biosynthesis of 7S,14S-diHDHA implicates 15-Lipoxygenase-2 in biosynthesis of resolvin D5, *J Lipid Res*.
[37] Maas, R. L., and Brash, A. R. (1983) Evidence for a lipoxygenase mechanism in the biosynthesis of epoxide and dihydroxy leukotrienes from 15(S)-hydroperoxyicosatetraenoic acid by human platelets and porcine leukocytes, *Proc Natl Acad Sci U S A 80*, 2884-2888.
[38] Serhan, C. N., Dalli, J., Karamnov, S., Choi, A., Park, C. K., Xu, Z. Z., Ji, R. R., Zhu, M., and Petasis, N. A. (2012) Macrophage proresolving mediator maresin 1 stimulates tissue regeneration and controls pain, *Faseb Journal 26*, 1755-1765.
[39] Butovich, I. A. (2006) A one-step method of 10,17-dihydro(pero)xydocosahexa-4Z,7Z,11E,13Z,15E,19Z-enoic acid synthesis by soybean lipoxygenase, *J Lipid Res 47*, 854-863.
[40] Green, A. R., Freedman, C., Tena, J., Tourdot, B. E., Liu, B., Holinstat, M., and Holman, T. R. (2018) 5 S,15 S-Dihydroperoxyeicosatetraenoic Acid (5,15-diHpETE) as a Lipoxin Intermediate: Reactivity and Kinetics with Human Leukocyte 5-Lipoxygenase, Platelet 12-Lipoxygenase, and Reticulocyte 15-Lipoxygenase-1, *Biochemistry 57*, 6726-6734.
[41] Banaszak, L., Winter, N., Xu, Z., Bernlohr, D. A., Cowan, S., and Jones, T. A. (1994) Lipid-binding proteins: a family of fatty acid and retinoid transport proteins, *Adv Protein Chem 45*, 89-151.
[42] Wecksler, A. T., Kenyon, V., Deschamps, J. D., and Holman, T. R. (2008) Substrate specificity changes for human reticulocyte and epithelial 15-lipoxygenases reveal allosteric product regulation, *Biochemistry 47*, 7364-7375.

[43] Minor, W., Steczko, J., Boguslaw, S., Otwinowski, Z., Bolin, J. T., Walter, R., and Axelrod, B. (1996) Crystal Structure of Soybean Lipoxygenase L-1 at 1.4 A Resolution, *Biochemistry 35*, 10687-10701.
[44] Prigge, S. T., Boyington, J. C., Gaffney, B. J., and Amzel, L. M. (1996) Structure Conservation in Lipoxygenases - Structural Analysis of Soybean Lipoxygenase-1 and Modeling of Human Lipoxygenases, *Proteins 24*, 275-291.
[45] Chen, X. S., and Funk, C. D. (1993) Structure-function properties of human platelet 12-lipoxygenase: chimeric enzyme and in vitro mutagenesis studies, *FASEB J 7*, 694-701.
[46] Kutzner, L., Goloshchapova, K., Heydeck, D., Stehling, S., Kuhn, H., and Schebb, N. H. (2017) Mammalian ALOX15 orthologs exhibit pronounced dual positional specificity with docosahexaenoic acid, *Biochim Biophys Acta Mol Cell Biol Lipids 1862*, 666-675.
[47] Freedman, C., Tran, A., Tourdot, B. E., Kalyanaraman, C., Perry, S., Holinstat, M., Jacobson, M. P., and Holman, T. R. (2020) Biosynthesis of the Maresin Intermediate, 13S,14S-Epoxy-DHA, by Human 15-Lipoxygenase and 12-Lipoxygenase and Its Regulation through Negative Allosteric Modulators, *Biochemistry 59*, 1832-1844.
[48] Tsai, W. C., Gilbert, N. C., Ohler, A., Armstrong, M., Perry, S., Kalyanaraman, C., Yasgar, A., Rai, G., Simeonov, A., Jadhav, A., Standley, M., Lee, H. W., Crews, P., Iavarone, A. T., Jacobson, M. P., Neau, D. B., Offenbacher, A. R., Newcomer, M., and Holman, T. R. (2021) Kinetic and structural investigations of novel inhibitors of human epithelial 15-lipoxygenase-2, *Bioorg Med Chem 46*, 116349.
[49] Saam, J., Ivanov, I., Walther, M., Holzhutter, H. G., and Kuhn, H. (2007) Molecular dioxygen enters the active site of 12/15-lipoxygenase via dynamic oxygen access channels, *Proc Natl Acad Sci U S A 104*, 13319-13324.
[50] Knapp, M. J., and Klinman, J. P. (2003) Kinetic Studies of Oxygen Reactivity in Soybean Lipoxygenase-1, *Biochemistry 42*, 11466-11475.
[51] Collazo, L., and Klinman, J. P. (2016) Control of the Position of Oxygen Delivery in Soybean Lipoxygenase-1 by Amino Acid Side Chains within a Gas Migration Channel, *J Biol Chem 291*, 9052-9059.
[52] Morita, E., Schroder, J. M., and Christophers, E. (1990) Identification of a novel and highly potent eosinophil chemotactic lipid in human eosinophils treated with arachidonic acid, *J Immunol 144*, 1893-1900.
[53] Turk, J., Maas, R. L., Brash, A. R., Roberts, L. J., 2nd, and Oates, J. A. (1982) Arachidonic acid 15-lipoxygenase products from human eosinophils, *J Biol Chem 257*, 7068-7076.
[54] Mainka, M., George, S., Angioni, C., Ebert, R., Goebel, T., Kampschulte, N., Krommes, A., Weigert, A., Thomas, D., Schebb, N. H., Steinhilber, D., and Kahnt, A. S. (2022) On the biosynthesis of specialized pro-resolving mediators in human neutrophils and the influence of cell integrity, *Biochim Biophys Acta Mol Cell Biol Lipids 1867*, 159093.